

COMMUNICATION

Highly Emissive Self-Trapped Excitons in Fully Inorganic Zero-Dimensional Tin Halides

Bogdan M. Benin,[†] Dmitry N. Dirin,[†] Viktoriia Morad, Michael Wörle, Sergii Yakunin, Gabriele Rainò, Olga Nazarenko, Markus Fischer, Ivan Infante, and Maksym V. Kovalenko^{*}

Abstract: The spatial localization of charge carriers to promote the formation of bound excitons and concomitantly enhance radiative recombination has long been a goal for luminescent semiconductors. Zero-dimensional materials structurally impose carrier localization and result in the formation of localized Frenkel excitons. Here we report that the fully inorganic, perovskite-derived zero-dimensional Sn(II) material Cs_4SnBr_6 exhibits room temperature, broad-band photoluminescence centred at 540 nm with a quantum yield (QY) of $15\pm 5\%$. A series of analogous compositions following the general formula $\text{Cs}_{4-x}\text{A}_x\text{Sn}(\text{Br}_{1-y}\text{I}_y)_6$ ($\text{A} = \text{Rb}, \text{K}; x \leq 1, y \leq 1$) can be prepared. The emission of these materials ranges from 500 nm to 620 nm with the possibility to compositionally tune the Stokes shift and the self-trapped exciton emission bands.

Interest in low-dimensional metal-halide semiconductors,^[1] and ultimately their zero-dimensional (0D) counterparts,^[2] has been spurred by the increasing interest in 3D lead halide perovskites.^[3] In recent years, lead-halide perovskites have risen to prominence in the field of optoelectronics with their use in full-color imaging,^[4] photodetection,^[5] X-ray imaging,^[6] hard-radiation detection,^[7] solar cells,^[8] and light-emitting diodes,^[9] owing to their defect-tolerant photophysics and charge transport.^[10]

As the dimensionality decreases, the metal halide octahedra become progressively less connected and the optical and electrical properties shift away from those of a delocalized, 3D network towards 0D, molecular-like, isolated octahedra. In such structures, self-trapped excitons (STEs) form due to the local deformation of the crystal lattice upon photoexcitation. This strong spatial localization, and the absence of electronic trapping processes that are inherent in electronically extended (higher-dimensionality) solids, favors radiative recombination. Previously, the spatial confinement of carriers in 3D perovskites has been attained through crystal size control at the nanoscale (*i.e.* top-

down and bottom-up synthesis of nanocrystals).^[11] In the case of 0D materials, such elaborate crystal size engineering is not required as the optical properties are instead governed by their structural dimensionality. Highly localized Frenkel-like excitons are formed instead of Wannier-Mott type excitons.

The library of 0D metal halides with octahedral building units includes both lead-based and lead-free compounds: Ti(IV),^[12] Hf(IV),^[13] Zr(IV),^[14] Pd(IV),^[15] Pb(II),^[16] Sn(IV),^[17] Te(IV),^[18] Sb(III),^[19] and Bi(III).^[20] However, only several of these examples exhibit photoluminescence (PL) at room temperature (RT); and this emission is seldom characterized by a high PL quantum yield (QY). The first examples with high QYs in excess of 50% were demonstrated only recently: $(\text{C}_4\text{N}_2\text{H}_{14}\text{Br})_4\text{SnBr}_6$ (QY = $95\pm 5\%$) and $(\text{C}_4\text{N}_2\text{H}_{14}\text{Br})_4\text{SnI}_6$ (QY = $75\pm 4\%$).^[21] Both structures are constructed from disconnected $[\text{SnX}_6]^{4-}$ octahedra, separated by large organic cations with a distance of >1 nm between Sn^{2+} centers.

Given the high PL QY of these hybrid materials and their novel approach towards exciton localization, we chose, herein, to pursue fully inorganic analogues such as Cs_4SnBr_6 . While several studies have reported on the structure and basic properties of Cs_4SnBr_6 , none have observed PL at RT.^[22] Recently, calculations have shown that the Cs_4SnBr_6 phase should have a bandgap of 3.37 eV.^[23] We prepared $\text{Cs}_{4-x}\text{A}_x\text{Sn}(\text{Br}_{1-y}\text{I}_y)_6$ ($\text{A} = \text{Rb}, \text{K}$) materials using a simple solid-state “heat-and-beat” approach, characterized them structurally and found them to be luminescent at RT.

According to the $\text{CsBr}-\text{SnBr}_2$ pseudo-binary phase diagram (Fig. 1a), Cs_4SnBr_6 melts incongruently and competes with the decomposition into the black CsSnBr_3 and CsBr . Therefore, phase pure Cs_4SnBr_6 cannot be obtained by cooling from a melt of this composition. Instead, solid pellets of a mixture of CsBr (4.5 eq.) and SnBr_2 (1 eq.) were repeatedly heated to 350 °C for 60 hours and reground in a glovebox between heating cycles. The highlighted green region in Fig. 1a represents the experimental conditions that were found to yield the purest materials, *i.e.* at temperatures below the decomposition point of Cs_4SnBr_6 (Fig. S1,2; Table S1,2). Single crystals of Cs_4SnBr_6 were obtained by tempering a solid pellet at 350 °C. Cs_4SnBr_6 crystallizes in a trigonal crystal system (R-3c space group, Fig. 1b, Table S3-9), wherein $[\text{SnBr}_6]^{4-}$ octahedra are separated by Cs^+ cations. The Cs^+ cations occupy two distinct crystallographic positions (Fig. S3).

Unlike the isostructural Cs_4PbBr_6 , which shows narrow excitonic PL only at low temperatures and at wavelengths <400 nm,^[16] Cs_4SnBr_6 exhibits broad-band green-yellow PL at RT from STEs (peak maximum at 540 nm, Fig. 1c). Upon measuring the PL excitation (PLE) and absorption spectra it was found that Cs_4SnBr_6 resembled a molecular material with a sharp excitation peak at 340 nm yielding a large Stokes shift of *ca.* 1.2 eV (Fig. S4) A PLQY of $15\pm 5\%$ was measured at RT. PLE and PL spectra were found to be tunable through the partial substitution of both A-site cations (Cs with Rb, K) and the halide anions (Br with I).

[a] B. M. Benin,^[†] Dr. D. N. Dirin,^[†] V. Morad, Dr. M. Wörle, Dr. S. Yakunin, Dr. G. Rainò, O. Nazarenko, M. Fischer, Prof. Dr. M. V. Kovalenko
 Laboratory of Inorganic Chemistry, ETH Zürich
 CH-8093 Zürich, Switzerland
 E-mail: mvkovalenko@ethz.ch

B. M. Benin, Dr. D. N. Dirin, V. Morad, Dr. Dr. S. Yakunin, Dr. G. Rainò, O. Nazarenko, Prof. Dr. M. V. Kovalenko
 Laboratory for Thin Films and Photovoltaics, Empa – Swiss Federal Laboratories for Materials
 CH-8600 Dübendorf, Switzerland

[b] Dr. I. Infante
 Department of Theoretical Chemistry, Faculty of Science, Vrije Universiteit Amsterdam, de Boelelaan 1083, 1081 HV Amsterdam, The Netherlands

[+] Equal contribution.
 Supporting information for this article is given via a link at the end of the document.

COMMUNICATION

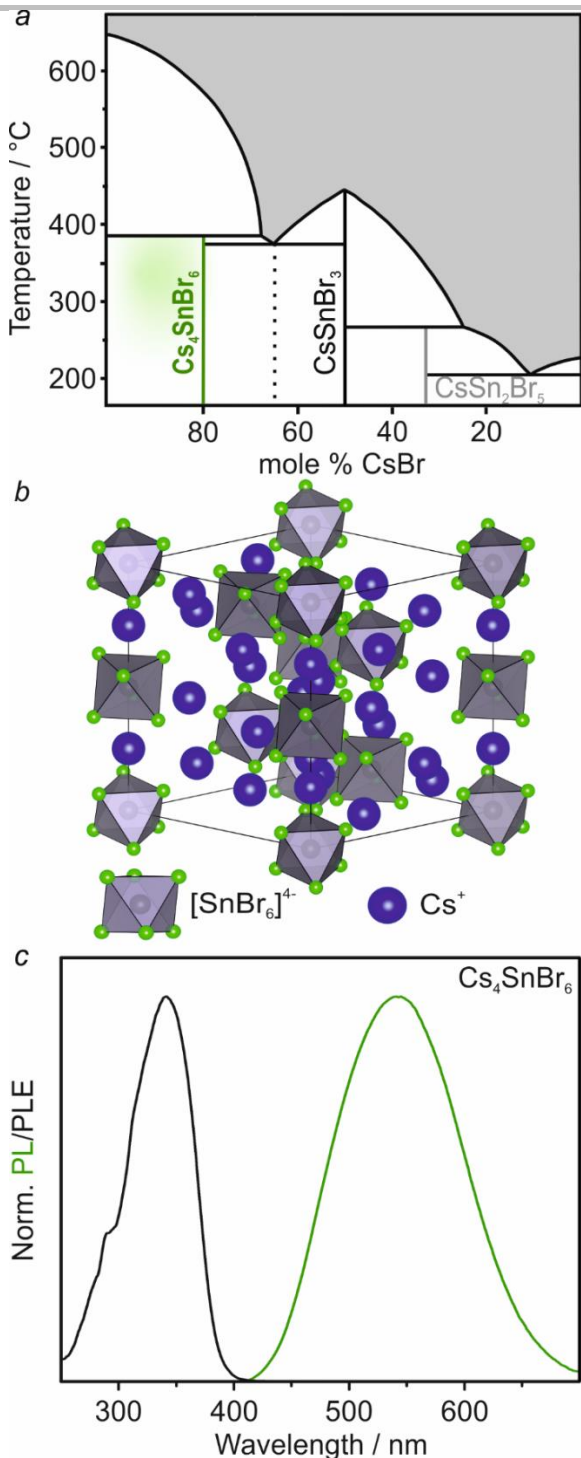


Figure 1. (a) The pseudo-binary $\text{CsBr}-\text{SnBr}_2$ phase diagram.^[22a] The highlighted green region represents the experimental conditions found to yield the purest Cs_4SnBr_6 material. (b) The crystal structure of Cs_4SnBr_6 viewed along the (111) axis with $[\text{SnBr}_6]^{4-}$ octahedra (grey with green bromine atoms) separated by Cs^+ cations (blue). (c) PL and PLE spectra for Cs_4SnBr_6 (at RT).

Na was not observed to substitute Cs (Fig. S5).

In $(\text{C}_4\text{N}_2\text{H}_{14}\text{Br})_4\text{SnX}_6$ ($\text{X} = \text{Br}/\text{I}$),^[21] the addition of iodide redshifts both the excitation and STE emission spectra. Similarly, the PL of Cs_4SnX_6 shifts to 620 nm (orange emission) at a Br:I ratio of ca. 1:1 (Fig. 2a). In agreement with Vegard's law, a linear

change in both the a and c lattice parameters was observed over the range of compositions from Cs_4SnBr_6 to Cs_4SnI_6 (Fig. S6,7; Table S10,11). Samples with greater than 50% substitution by iodide, however, did not exhibit PL at RT and were not investigated further.

While bromide and iodide occupy the same general position within the structure of Cs_4SnBr_6 , Rb^+ and K^+ could potentially substitute two distinct crystallographic positions of Cs^+ (Fig. S3). Substitution by Rb^+ or K^+ occurred only on the $\text{Cs}(2)$ site (1/4 of all Cs, six-fold coordination, Fig. 2b, S8; Table S12,13), which explains the observed experimental 25%-limit for substitution (Fig. S9). Plotting the lattice constants against the molar fractions of K^+ or Rb^+ ions, estimated from the Rietveld refinement and energy-dispersive X-ray spectroscopy (EDS), yields a seemingly linear trend for the c parameter, in agreement with Vegard's law, whereas the a parameter increases only slightly (Fig. 2c, S9-11). The site affected is part of an infinite chain of $[\text{SnBr}_6]^{4-}$ octahedra separated by $\text{Cs}/\text{Rb}/\text{K}$ ions. Since the chain is oriented parallel to the c -axis, substitution by Rb or K will cause the largest effect along this axis resulting in a decrease in the c parameter.

The substitution of Cs^+ by Rb^+ or K^+ results in a blue-shift of the PL maximum. This shift is dependent on both the degree of substitution and on the identity of the substituting cation. For 25% substitution, Rb^+ shifts the PL peak to 519 nm, whereas K^+ yields a PL peak at 500 nm (Fig. 2d). Strikingly, the PLE remains unaffected. The same scenario was observed for the other examined Br:I ratios (ca. 5:1, 2:1, 1:1, Fig. 2e, S12; Table S14,15).

Temperature-dependent PL spectra were measured down to 6 K (Fig. S13,14). It was found that the PL intensity increased with decreasing temperature and, in the case of Cs_4SnBr_6 , the emission intensity reached a maximum at ca. 200 K. Given a RT QY of $15 \pm 5\%$, the QY of Cs_4SnBr_6 is estimated to be near-unity at 200 K (Fig. S15a). At 6 K, no higher-energy emission, *i.e.* from free excitons, could be observed in Cs_4SnBr_6 or $\text{Cs}_4\text{SnBr}_3\text{I}_3$ (Fig. S14,15b).

The time-resolved PL (TRPL) of Cs_4SnBr_6 at RT exhibits a monoexponential decay with an average lifetime of 540 ns (Fig. S16). TRPL decays were then recorded at 200 K (the temperature that corresponds to highest QY, Fig. 2f, S15), and it was observed that the lifetime increased to 1381 ns (1424 ns for K-substitution), while remaining monoexponential (Fig. 2f). Substitution with iodide accelerated the average lifetime (600 ns at 200 K for $\text{Cs}_4\text{SnBr}_3\text{I}_3$, Fig. 2f; see Fig. S16b for RT comparison). Additionally, the radiative lifetime was found to be insensitive towards dilution with CsBr, excitation intensity, crystallinity and encapsulation within a UV curable epoxy (Fig. S16c, d) indicating a lack of surface effects on PL properties in these 0D materials.

Broad-band, strongly Stokes shifted emission with relatively long radiative lifetimes indicates the formation of STEs (Figure 3a). As in molecular complexes and similarly small entities, structural changes occur between the ground state and the excited state. Emission from STEs is then somewhat similar to an indirect-gap optical transition since coupling to phonons is required.^[24] Besides 0D-tin halides,^[21b] emission from STEs has also been observed in 1D- and 2D-layered materials.^[25]

To rationalize the effect of A-site substitution observed in these materials, calculations of the partial density of states (DOS) by density functional theory (DFT) were utilized (Fig. 3b, S17; Table S16).

COMMUNICATION

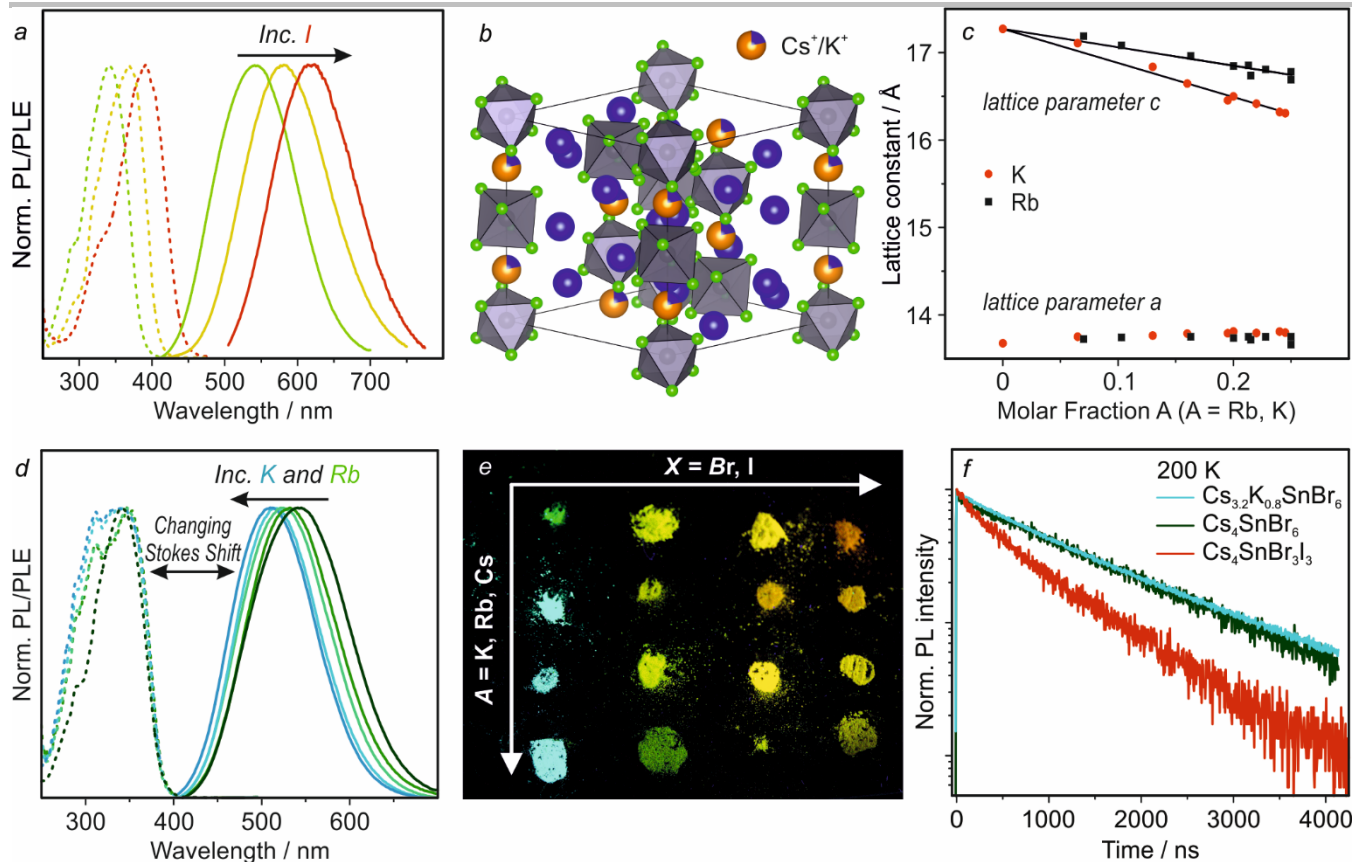


Figure 2. Structural and optical characterization of $\text{Cs}_{4-x}\text{A}_x\text{Sn}(\text{Br},\text{I})_6$ compounds ($\text{A}=\text{K}, \text{Rb}$). (a) PL and PLE spectra of $\text{Cs}_4\text{Sn}(\text{Br},\text{I})_6$. (b) Crystal structure of $\text{Cs}_{3.2}\text{K}_{0.8}\text{SnBr}_6$ determined by Rietveld refinement. (c) The change in the a and c lattice parameters upon Cs^+ substitution by Rb^+ and K^+ . (d) PL and PLE spectra for Rb^+ or K^+ substituted compounds. (e) Image of $\text{Cs}_{4-x}\text{A}_x\text{Sn}(\text{Br},\text{I})_6$ powders under 365 nm UV light. (f) TRPL of Cs_4SnBr_6 , $\text{Cs}_{3.2}\text{K}_{0.8}\text{SnBr}_6$, and $\text{Cs}_4\text{SnBr}_3\text{I}_3$ at 200 K.

A $1\times 1\times 1$ unit cell (66 atoms) was used as a model system for Cs_4SnBr_6 , $\text{Cs}_3\text{RbSnBr}_6$, and $\text{Cs}_3\text{KSnBr}_6$ materials. The electronic states were found to be highly localized in all three compositions and the band gap was found to consist of Sn 5s, Br 5p (conduction band/LUMO) and Sn 5p, Br 5p orbitals (valence band/HOMO). A-cation orbitals do not significantly contribute to HOMO and LUMO states (Fig. S17). This is corroborated by the experiment given that A-site substitution did not substantially affect the PLE spectra.

It was previously shown that both tin- and lead-halide octahedra distort significantly upon photoexcitation in low dimensional materials.^[26] By modeling the excited state and ground state geometries, we find that the extent of distortion was the principle reason for the Stokes shift (Fig. 3b). A pseudo-Jahn-Teller distortion was observed with elongation of up to 17% in the axial Sn-Br bonds, and a contraction of up to 7% in the equatorial bonds. This distortion was found to be greatest in Cs_4SnBr_6 and decreased from Cs^+ to Rb^+ to K^+ (Table S17). In other words, the energy required for distortion correlates well with the measured Stokes shift. Larger distortion is allowed by greater distance between the octahedra; primarily along the c -axis. The ratio between the lengths of the c - and a -axes was found to correlate most strongly with PL energy, experimentally and in calculations (Fig. 3c). On the other hand, isotropic changes to the unit cell (i.e. contraction during cooling) do not affect the PL (Table S18).

In summary, several new 0D Sn-halides with the general formula $\text{Cs}_{4-x}\text{A}_x\text{Sn}(\text{Br}_1\text{-l}_y)_6$ have been found to exhibit broad-band RT PL that is tunable from 500 nm to 620 nm. The PL peak position and Stokes shifts can be concomitantly adjusted by the substitution of Cs^+ with either Rb^+ or K^+ as well as Br by I. PL properties were rationalized by the DFT analysis of STEs. Future studies might concern applications of such materials in luminescent solar concentrators and light emitting devices, harnessing their structural tunability and fully-inorganic compositions.

Experimental Section

Materials and methods are included in the supplementary information. Further details on the crystal structure investigation(s) may be obtained from the Fachinformationszentrum Karlsruhe, 76344 Eggenstein-Leopoldshafen, Germany (fax: (+49)7247-808-666; e-mail: crysdata@fiz-karlsruhe.de), on quoting the depositary number CSD- 434641, 434642, 434643, 434644, 434645, 434646, and 434647.

COMMUNICATION

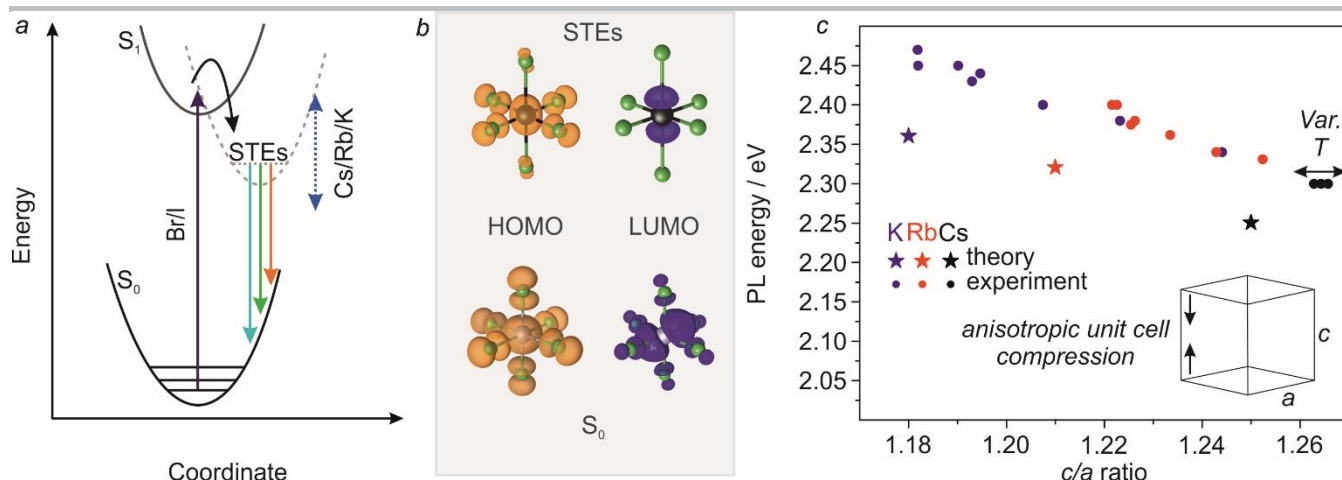


Figure 3. (a) Generic configurational coordinate diagram depicting formation illustrating the origin of STE PL in $\text{Cs}_{4-x}\text{Ax}\text{Sn}(\text{Br}_{1-y}\text{ly})_6$. (b) Ground state and excited state (STE) HOMOs and LUMOs. (c) Experimental and theoretical results demonstrating that PL energy varies linearly with the ratio of c-axis to a-axis length. Variable temperature measurements (three data points; black circles) are plotted for Cs_4SnBr_6 at 100 K, 200 K, and 273 K.

Acknowledgements

We thank Dr. F. Krumeich for EDS measurements and acknowledge the support of the Scientific Center for Optical and Electron Microscopy (ScopeM) of the Swiss Federal Institute of Technology ETHZ. This work was financially supported by the European Union through the FP7 (ERC Starting Grant NANOSOLID, GA No. 306733) and through the Horizon-2020 (Marie-Skłodowska Curie ITN network PHONSI, H2020-MSCA-ITN-642656). Authors thank IBM-Zurich Research, in particular Dr. T. Stöferle and Dr. R. F. Mahrt, for support with low-temperature PL experiments. I.I. would like to thank The Netherlands Organization of Scientific Research (NWO) for providing financial support within the Innovational Research Incentive (Vidi) Scheme (Grant no. 723.013.002). DFT calculations were carried out on the Dutch national e-infrastructure with the support of SURF Cooperative.

Keywords: perovskites • luminescence • phase diagram • self-trapped excitons • solid-state synthesis

- [1] a) D. B. Mitzi, C. A. Felid, W. T. A. Harrison, A. M. Guloy, *Nature* **1994**, *369*, 467–469; b) D. B. Mitzi, K. Liang, S. Wang, *Inorg. Chem.* **1998**, *37*, 321–327; c) Z. Xu, D. B. Mitzi, *Inorg. Chem.* **2003**, *42*, 6589–6591; d) L. Pedesseau, D. Sapori, B. Traore, R. Robles, H. H. Fang, M. A. Loi, H. Tsai, W. Nie, J. C. Blancon, A. Neukirch, S. Tretiak, A. D. Mohite, C. Katan, J. Even, M. Kepenekian, *ACS Nano* **2016**, *10*, 9776–9786; e) L. Mao, H. Tsai, W. Nie, L. Ma, J. Im, C. C. Stoumpos, C. D. Malliakas, F. Hao, M. R. Wasielewski, A. D. Mohite, M. G. Kanatzidis, *Chem. Mater.* **2016**, *28*, 7781–7792; f) C. C. Stoumpos, D. H. Cao, D. J. Clark, J. Young, J. M. Rondinelli, J. I. Jang, J. T. Hupp, M. G. Kanatzidis, *Chem. Mater.* **2016**, *28*, 2852–2867; g) H. Tsai, W. Nie, J. C. Blancon, C. C. Stoumpos, R. Asadpour, B. Harutyunyan, A. J. Neukirch, R. Verduzco, J. J. Crochet, S. Tretiak, L. Pedesseau, J. Even, M. A. Alam, G. Gupta, J. Lou, P. M. Ajayan, M. J. Bedzyk, M. G. Kanatzidis, *Nature* **2016**, *536*, 312–316; h) L. Mao, Y. Wu, C. C. Stoumpos, M. R. Wasielewski, M. G. Kanatzidis, *J. Am. Chem. Soc.* **2017**, *139*, 5210–5215; i) L. Mao, Y. Wu, C. C. Stoumpos, B. Traore, C. Katan, J. Even, M. R. Wasielewski, M. G. Kanatzidis, *J. Am. Chem. Soc.* **2017**, *139*, 11956–11963; j) D. H. Cao, C. C. Stoumpos, T. Yokoyama, J. L. Logsdon, T.-B. Song, O. K. Farha, M. R. Wasielewski, J. T. Hupp, M. G. Kanatzidis, *ACS Energy Lett.* **2017**, *2*, 982–990; k) C. M. M. Soe, C. C. Stoumpos, M. Kepenekian, B. Traore, H. Tsai, W. Nie, B. Wang, C. Katan, R. Seshadri, A. D. Mohite, J. Even, T. J. Marks, M. G. Kanatzidis, *J. Am. Chem. Soc.* **2017**, *139*, 16297–16309; l) O. Nazarenko, M. R. Kotyra, M. Worle, E. Cuervo-Reyes, S. Yakunin, M. V. Kovalenko, *Inorg. Chem.* **2017**, *56*, 11552–11564; m) C. C. Stoumpos, L. Mao, C. D. Malliakas, M. G. Kanatzidis, *Inorg. Chem.* **2017**, *56*, 56–73; n) O. Nazarenko, M. R. Kotyra, S. Yakunin, M. Aebl, G. Raino, B. M. Benin, M. Worle, M. V. Kovalenko, *J. Am. Chem. Soc.* **2018**, *140*, 3850–3853; o) M. D. Smith, H. I. Karunadasa, *Acc. Chem. Res.* **2018**, *51*, 619–627.
- [2] a) M. I. Saidaminov, O. F. Mohammed, O. M. Bakr, *ACS Energy Lett.* **2017**, *2*, 889–896; b) H. Lin, C. Zhou, Y. Tian, T. Siegrist, B. Ma, *ACS Energy Lett.* **2017**, *3*, 54–62; c) Q. A. Akkerman, A. L. Abdelhady, L. Manna, *J. Phys. Chem. Lett.* **2018**, *9*, 2326–2337.
- [3] a) M. A. Green, A. Ho-Baillie, H. J. Snaith, *Nat. Photonics* **2014**, *8*, 506–514; b) J. S. Manser, J. A. Christians, P. V. Kamat, *Chem. Rev.* **2016**, *116*, 12956–13008; c) Q. A. Akkerman, G. Raino, M. V. Kovalenko, L. Manna, *Nat. Mater.* **2018**, *17*, 394–405.
- [4] S. Yakunin, Y. Shynkarenko, D. N. Dirin, I. Cherniukh, M. V. Kovalenko, *NPG Asia Mater.* **2017**, *9*, 1–7.
- [5] a) X. Hu, X. Zhang, L. Liang, J. Bao, S. Li, W. Yang, Y. Xie, *Adv. Funct. Mater.* **2014**, *24*, 7373–7380; b) L. Dou, Y. M. Yang, J. You, Z. Hong, W. H. Chang, G. Li, Y. Yang, *Nat. Commun.* **2014**, *5*, 1–6.
- [6] S. Yakunin, M. Sytnyk, D. Kriegner, S. Shrestha, M. Richter, G. J. Matt, H. Azimi, C. J. Brabec, J. Stangl, M. V. Kovalenko, W. Heiss, *Nat. Photonics* **2015**, *9*, 444–449.
- [7] a) C. C. Stoumpos, C. D. Malliakas, J. A. Peters, Z. Liu, M. Sebastian, J. Im, T. C. Chasapis, A. C. Wibowo, D. Y. Chung, A. J. Freeman, B. W. Wessels, M. G. Kanatzidis, *Cryst. Growth Des.* **2013**, *13*, 2722–2727; b) S. Yakunin, D. N. Dirin, Y. Shynkarenko, V. Morad, I. Cherniukh, O. Nazarenko, D. Kreil, T. Nauser, M. V. Kovalenko, *Nat. Photonics* **2016**, *10*, 585–589.
- [8] a) M. M. Lee, J. Teuscher, T. Miyasaka, T. N. Murakami, H. J. Snaith, *Science* **2012**, *338*, 643–647; b) J. Burschka, N. Pellet, S. J. Moon, R. Humphry-Baker, P. Gao, M. K. Nazeeruddin, M. Grätzel, *Nature* **2013**, *499*, 316–319.
- [9] Z.-K. Tan, R. S. Moghaddam, M. L. Lai, P. Docampo, R. Higler, F. Deschler, M. Price, A. Sadhanala, L. M. Pazos, D. Credgington, F. Hanusch, T. Bein, H. J. Snaith, R. H. Friend, *Nat. Nanotechnol.* **2014**, *9*, 687–692.
- [10] a) R. E. Brandt, V. Stevanović, D. S. Ginley, T. Buonassisi, *MRS Commun.* **2015**, *5*, 265–275; b) O. Yaffe, Y. Guo, L. Z. Tan, D. A. Egger, T. Hull, C. C. Stoumpos, F. Zheng, T. F. Heinz, L. Kronik, M. G. Kanatzidis, J. S. Owen, A. M. Rappe, M. A. Pimenta, L. E. Brus, *Phys.*

COMMUNICATION

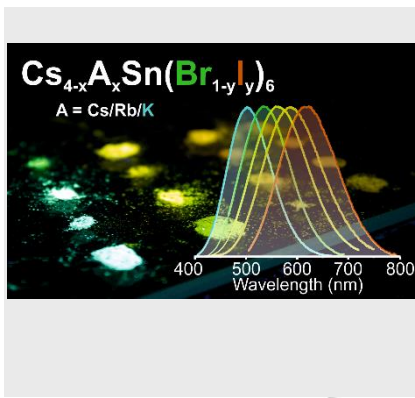
- Rev. Lett.* **2017**, *118*, 136001; c) K. Miyata, T. L. Atallah, X.-Y. Zhu, *Sci. Adv.* **2017**, *3*, e1701469.
- [11] a) L. C. Schmidt, A. Pertegas, S. Gonzalez-Carrero, O. Malinkiewicz, S. Agouram, G. Minguez Espallargas, H. J. Bolink, R. E. Galian, J. Perez-Prieto, *J. Am. Chem. Soc.* **2014**, *136*, 850-853; b) L. Protesescu, S. Yakunin, M. I. Bodnarchuk, F. Krieg, R. Caputo, C. H. Hendon, R. X. Yang, A. Walsh, M. V. Kovalenko, *Nano Lett.* **2015**, *15*, 3692-3696; c) D. N. Dirin, L. Protesescu, D. Trummer, I. V. Kochetygov, S. Yakunin, F. Krumeich, N. P. Stadie, M. V. Kovalenko, *Nano Lett.* **2016**, *16*, 5866-5874; d) Q. A. Akkerman, S. G. Motti, A. R. Srimath Kandada, E. Mosconi, V. D'Innocenzo, G. Bertoni, S. Marras, B. A. Kamino, L. Miranda, F. De Angelis, A. Petrozza, M. Prato, L. Manna, *J. Am. Chem. Soc.* **2016**, *138*, 1010-1016; e) H. Huang, Q. Xue, B. Chen, Y. Xiong, J. Schneider, C. Zhi, H. Zhong, A. L. Rogach, *Angew. Chem. Int. Ed. Engl.* **2017**, *56*, 9571-9576; f) L. Protesescu, S. Yakunin, O. Nazarenko, D. N. Dirin, M. V. Kovalenko, *ACS Appl. Nano Mater.* **2018**, *1*, 1300-1308.
- [12] M. Chen, M.-G. Ju, A. D. Carl, Y. Zong, R. L. Grimm, J. Gu, X. C. Zeng, Y. Zhou, N. P. Padture, *Joule* **2018**, *2*, 558-570.
- [13] a) B. Kang, K. Biswas, *J. Phys. Chem. C* **2016**, *120*, 12187-12195; b) R. Král, V. Babin, E. Mihóková, M. Buryi, V. V. Laguta, K. Nitsch, M. Nikl, *J. Phys. Chem. C* **2017**, *121*, 12375-12382.
- [14] K. Saeki, Y. Fujimoto, M. Koshimizu, D. Nakauchi, H. Tanaka, T. Yanagida, K. Asai, *Jpn. J. Appl. Phys.* **2018**, *57*, 1-4.
- [15] N. Sakai, A. A. Haghhighirad, M. R. Filip, P. K. Nayak, S. Nayak, A. Ramadan, Z. Wang, F. Giustino, H. J. Snaith, *J. Am. Chem. Soc.* **2017**, *139*, 6030-6033.
- [16] M. Nikl, E. Mihokova, K. Nitsch, F. Somma, C. Giampaolo, G. P. Pazzi, P. Fabeni, S. Zazubovich, *Chem. Phys. Lett.* **1999**, *306*, 280-284.
- [17] a) B. Lee, C. C. Stoumpos, N. Zhou, F. Hao, C. Malliakas, C. Y. Yeh, T. J. Marks, M. G. Kanatzidis, R. P. Chang, *J. Am. Chem. Soc.* **2014**, *136*, 15379-15385; b) A. Kaltzoglou, M. Antoniadou, A. G. Kontos, C. C. Stoumpos, D. Perganti, E. Siranidi, V. Raptis, K. Trohidou, V. Psycharis, M. G. Kanatzidis, P. Falaras, *J. Phys. Chem. C* **2016**, *120*, 11777-11785.
- [18] a) R. Wernicke, H. Kupka, W. Ensslin, H.-H. Schmidtke, *Chem. Phys.* **1980**, *47*, 235-244; b) G. Blasse, G. J. Dirksen, W. Abriel, *Chem. Phys. Lett.* **1987**, *136*, 460-464; c) T. V. Sedakova, A. G. Mirochnik, V. E. Karasev, *Opt. Spectrosc.* **2011**, *110*, 755-761; d) B. V. Bukvetskii, T. V. Sedakova, A. G. Mirochnik, *Russ. J. Coord. Chem.* **2012**, *38*, 106-110.
- [19] a) T. V. Sedakova, A. G. Mirochnik, V. E. Karasev, *Opt. Spectrosc.* **2008**, *105*, 517-523; b) V. I. Vovna, A. A. Dotsenko, V. V. Korochentsev, O. L. Shcheka, I. S. Os'mushko, A. G. Mirochnik, T. V. Sedakova, V. I. Sergienko, *J. Mol. Struct.* **2015**, *1091*, 138-146; c) C. Zhou, M. Worku, J. Neu, H. Lin, Y. Tian, S. Lee, Y. Zhou, D. Han, S. Chen, A. Hao, P. I. Djurovich, T. Siegrist, M.-H. Du, B. Ma, *Chem. Mater.* **2018**, *30*, 2374-2378.
- [20] N. Elfaleh, S. Kamoun, *J. Organomet. Chem.* **2016**, *819*, 95-102.
- [21] a) C. Zhou, Y. Tian, Z. Yuan, H. Lin, B. Chen, R. Clark, T. Dilbeck, Y. Zhou, J. Hurley, J. Neu, T. Besara, T. Siegrist, P. Djurovich, B. Ma, *ACS Appl. Mater. Interfaces* **2017**, *9*, 44579-44583; b) C. Zhou, H. Lin, Y. Tian, Z. Yuan, R. Clark, B. Chen, L. J. van de Burgt, J. C. Wang, Y. Zhou, K. Hanson, Q. J. Meissner, J. Neu, T. Besara, T. Siegrist, E. Lambers, P. Djurovich, B. Ma, *Chem. Sci.* **2018**, *9*, 586-593.
- [22] a) R. H. Andrews, S. J. Clark, J. D. Donaldson, *J. Chem. Soc., Dalton Trans.* **1983**, 767-770; b) S. V. Myagkota, P. V. Savchin, A. S. Voloshinovskii, T. M. Demkiv, Y. V. Boiko, R. S. Vus, L. S. Demkiv, *Phys. Solid State* **2008**, *50*, 1473-1476.
- [23] M. Hu, C. Ge, J. Yu, J. Feng, *J. Phys. Chem. C* **2017**, *121*, 27053-27058.
- [24] K. Thirumal, W. K. Chong, W. Xie, R. Ganguly, S. K. Muduli, M. Sherburne, M. Asta, S. Mhaisalkar, T. C. Sum, H. S. Soo, N. Mathews, *Chem. Mater.* **2017**, *29*, 3947-3953.
- [25] a) E. R. Dohner, A. Jaffe, L. R. Bradshaw, H. I. Karunadasa, *J. Am. Chem. Soc.* **2014**, *136*, 13154-13157; b) Z. Yuan, C. Zhou, Y. Tian, Y. Shu, J. Messier, J. C. Wang, L. J. van de Burgt, K. Kountouriotis, Y. Xin, E. Holt, K. Schanze, R. Clark, T. Siegrist, B. Ma, *Nat. Commun.* **2017**, *8*, 1-7; c) M. D. Smith, B. L. Watson, R. H. Dauskardt, H. I. Karunadasa, *Chem. Mater.* **2017**, *29*, 7083-7087.
- [26] a) C. Zhou, H. Lin, H. Shi, Y. Tian, C. Pak, M. Shatruk, Y. Zhou, P. Djurovich, M. H. Du, B. Ma, *Angew. Chem. Int. Ed. Engl.* **2018**, *57*, 1021-1024; b) B. Kang, K. Biswas, *J. Phys. Chem. Lett.* **2018**, *9*, 830-836.

COMMUNICATION

Entry for the Table of Contents

COMMUNICATION

Fully inorganic, perovskite-derived zero-dimensional Cs_4SnBr_6 exhibits room temperature, broad-band photoluminescence from self-trapped excitons, centred at 540 nm with a quantum yield of $15\pm 5\%$ (298 K; near 100% at 200 K), and a large Stokes shift of ca. 1.2 eV. A compositional series, $\text{Cs}_{4-x}\text{A}_x\text{Sn}(\text{Br}_{1-y}\text{I}_y)_6$ ($\text{A} = \text{Rb}, \text{K}$; $x \leq 1, y \leq 1$), was obtained wherein the emission peak ranges from 500 nm to 620 nm.



Bogdan M. Benin,[†] Dmitry N. Dirlin,[†] Viktoria Morad, Michael Wörle, Sergii Yakunin, Gabriele Rainò, Olga Nazarenko, Markus Fischer, Ivan Infante, and Maksym V. Kovalenko*

Page No. – Page No.

Highly Emissive Self-Trapped Excitons in Fully Inorganic Zero-Dimensional Tin Halides